The Astrophysical Journal, 701:L83–L86, 2009 August 20 doi:10.1088/0004-637X/701/2/L83

MEASURING BLACK HOLE SPIN VIA THE X-RAY CONTINUUM-FITTING METHOD: BEYOND THE THERMAL DOMINANT STATE

James F. Steiner[1], Jeffrey E. McClintock[1], Ronald A. Remillard[2], Ramesh Narayan[1], and Lijun Gou[1]

[1] Harvard-Smithsonian Center for Astrophysics, 60 Garden Street, Cambridge, MA 02138, USA; jsteiner@cfa.harvard.edu

[2] MIT Kavli Institute for Astrophysics and Space Research, MIT, 70 Vassar Street, Cambridge, MA 02139, USA

Received 2009 May 5; accepted 2009 July 20; published 2009 August 4

ABSTRACT

All prior work on measuring the spins of stellar-mass black holes (BHs) via the X-ray continuum-fitting (CF) method has relied on the use of weakly Comptonized spectra obtained in the thermal dominant (TD) state. Using a self-consistent Comptonization model, we show that one can analyze spectra that exhibit strong power-law components and obtain values of the inner disk radius, and hence spin, that are consistent with those obtained in the TD state. Specifically, we analyze many *RXTE* spectra of two BH transients, H1743−322 and XTE J1550−564, and we demonstrate that the radius of the inner edge of the accretion disk remains constant to within a few percent as the strength of the Comptonized component increases by an order of magnitude, i.e., as the fraction of the thermal seed photons that are scattered approaches 25%. We conclude that the CF method can be applied to a much wider body of data than previously thought possible, and to sources that have never been observed to enter the TD state (e.g., Cyg X-1).

Key words: accretion, accretion disks – black hole physics – stars: individual (H1743−322, XTE J1550−564) – X-rays: binaries

1. INTRODUCTION

Black holes (BHs) are completely described by only three quantities: mass, charge, and spin. In astrophysical settings, any net charge will rapidly neutralize, with the result that a stellar-mass BH is specified by just its mass and spin. BH spin is commonly expressed in terms of the dimensionless parameter $a_* \equiv cJ/GM^2$ with $|a_*| \leqslant 1$, where M and J are the BH mass and angular momentum, and c and G are the speed of light and Newton's constant, respectively. While mass measurements of stellar-mass BHs have been made for decades, the first spin measurements have been achieved only during the past three years (Shafee et al. 2006; McClintock et al. 2006; Liu et al. 2008; Gou et al. 2009; Miller et al. 2009, and references therein). Meanwhile, the spins of supermassive BHs also have been measured (Brenneman & Reynolds 2006; Miniutti et al. 2007). The only two methods presently available to measure BH spin are via modeling the thermal continuum spectrum of a BH accretion disk, as pioneered by Zhang et al. (1997), or by modeling the profile of a relativistically broadened Fe K fluorescence line, as demonstrated by Tanaka et al. (1995).

Spin is measured by estimating the inner radius of the accretion disk $R_{\rm in}$. One identifies $R_{\rm in}$ with the radius of the innermost stable circular orbit $R_{\rm ISCO}$, which is dictated by general relativity. $R_{\rm ISCO}/M$ is a monotonic function of a_*, decreasing from $6G/c^2$ to $1G/c^2$ as spin increases from $a_* = 0$ to $a_* = 1$ (Shapiro & Teukolsky 1983). This relationship between a_* and $R_{\rm ISCO}$ is the foundation of both methods of measuring spin.

In the continuum-fitting (CF) method, one determines $R_{\rm ISCO}$ by modeling the X-ray continuum spectrum, focusing on the thermal accretion-disk component. The observables are flux, temperature, distance D, inclination i, and mass M. To obtain reliable values of spin, it is essential to have accurate estimates for M, i, and D, which are typically derived from optical data.

The CF method has been applied only to spectral data obtained in the thermal dominant (TD) state (or very recently to a near-TD intermediate state; Gou et al. 2009). The TD state is chiefly characterized by the dominance of the soft, thermal disk component of emission. For a measure of this dominance and a review of BH states, see Remillard & McClintock (2006). The CF method has never been applied to the more Comptonized steep power-law (SPL) state, which is characterized by the coexistence of a strong power-law component with photon index $\Gamma > 2.4$ and a significant thermal component. Most models for the SPL state invoke Compton upscattering of thermal seed photons by coronal electrons as the mechanism that generates the power law. Herein, we employ a self-consistent Comptonized accretion-disk model that yields values of $R_{\rm in}$ for SPL-state spectra that are consistent with those obtained for TD-state spectra. This result greatly increases the reach of the CF method, allowing one to obtain reliable measurements of spin for a much wider body of data than previously supposed, and for sources that do not enter the TD state (e.g., Cyg X-1). Moreover, the success of this model supports the widely held assumption that Comptonization is the mechanism that generates the observed high-energy power-law component in SPL- and TD-state spectra.

Our full model of a Comptonized accretion disk is a convolution of the relativistic thin accretion-disk model KERRBB2 (Li et al. 2005; McClintock et al. 2006) and SIMPL, an empirical model that convolves a Comptonization Green's function with an arbitrary seed photon spectrum (Steiner et al. 2009). Both models are implemented in XSPEC (Arnaud 1996). SIMPL, with only two parameters, ensures photon conservation and self-consistently generates the power-law component of the spectrum of an accreting BH using the accretion-disk component as input.

We have chosen to apply our spectral model to the two bright transient X-ray sources H1743−322 (hereafter H1743), which we feature, and XTE J1550−564 (hereafter J1550). Both transients are sources of large-scale relativistic jets and high-frequency quasi-periodic oscillations (QPOs) (Remillard & McClintock 2006, and references therein). For a detailed comparison of the spectral and timing characteristics of these very similar transients during their principal outbursts, see McClintock et al. (2009). Presently, the distance to J1550 is poorly constrained (see Orosz et al. 2002), and no useful distance estimate or dynamical information whatsoever is available for the

BH candidate H1743. Consequently, we cannot yet accurately estimate the spins of these BHs. In this work, we adopt fiducial values of M, i, and D. Of course, $R_{\rm in}$ (and a_*) depend strongly on these fiducial values. However, as we show in Section 3.3, for any reasonable range of these input parameters, the dependence of $R_{\rm in}$ on luminosity or on time during the outburst cycle is slight, which is an important conclusion of this work.

We show that the very widely used additive XSPEC models of Comptonization, namely the empirical model POWERLAW and the physical model COMPTT (Titarchuk 1994; Section 3), are inadequate for extracting measurements of spin from spectra with substantial power-law components. A self-consistent model such as SIMPL is required.

2. OBSERVATIONS AND ANALYSIS

We apply the model described below to the full archive of spectral data for the 2003 outburst of H1743 (the most intense observed for this source) and for all five outburst cycles of J1550 obtained using the *Rossi X-ray Timing Explorer*'s (*RXTE*'s) Proportional Counter Array (PCA; Swank 1999). We rely solely upon "standard 2" spectra obtained using the PCU-2 module, *RXTE*'s best-calibrated detector. All spectra have been binned into approximately half-day intervals, background subtracted, and have typical exposure times ∼3000 s. For the first 5 weeks of PCA observations (through 2003 May 1 UT), the detector was pointed 0.°32 from H1743. We have corrected the fluxes to full collimator transmission assuming a triangular response with FWHM = 1°. We applied similar collimator corrections (≈0.°1–0.°3) to three observations of J1550 performed on 1998 September 7–8 and 1999 January 5 UT.

A 1% systematic error has been included over all channels to account for uncertainties in the response of the detector (details on *RXTE*'s calibration can be found in Jahoda et al. 2006). As in our earlier work (e.g., McClintock et al. 2006), we have corrected for detector dead time while using contemporaneous Crab observations and the canonical Crab spectrum of Toor & Seward (1974) in order to calibrate the PCA effective area. The resultant pulse-height spectra are analyzed from 2.8–25 keV using XSPEC v12.5.0.

In XSPEC, the model we employ is PHABS (SIMPL⊗KERRBB2), where PHABS is a widely used model of low-energy photoabsorption. SIMPL redirects photons from the seed distribution, described here by the accretion-disk model KERRBB2, into a Compton power law. Like POWERLAW, SIMPL has just two parameters: (1) the fraction of seed photons $f_{\rm SC}$ scattered into the power law and (2) the photon power-law index Γ. SIMPL does not incorporate higher-order effects such as geometry-dependent scattering or reflection. The relativistic disk model KERRBB2 similarly has two fit parameters: (1) the spin parameter a_*, which we express equivalently in terms of $R_{\rm in}$ (Section 1), and (2) the mass accretion rate $\dot{M}$. From these two parameters, we compute the Eddington-scaled disk luminosity, $L_D(a_*, \dot{M})/L_{\rm Edd}$, where L_D is the luminosity of the seed photons and $L_{\rm Edd} \approx 1.3 \times 10^{38} M/M_\odot$ erg s^{-1} (Shapiro & Teukolsky 1983). The low-energy cutoff is parameterized in the PHABS component by the column density $N_{\rm H}$, which we fix at 2.2×10^{22} cm^{-2} for H1743 and 8×10^{21} cm^{-2} for J1550 (McClintock et al. 2009; Miller et al. 2003). We include an additional model component to account for disk-reflection using the XSPEC model SMEDGE for J1550, which was not required for H1743.

In our analyses described in Sections 3.1 and 3.2, we adopt the following dynamical model parameters: for H1743, $M = 10\ M_\odot$, $i = 60°$, and $D = 9.5$ kpc; and for J1550, $M = 10\ M_\odot$, $i = 70°$, and $D = 5$ kpc. The values for H1743 are chosen arbitrarily to place the maximum outburst disk luminosity at $L_D/L_{\rm Edd} \approx 0.7$, and those for J1550 are round numbers based on the model described in Orosz et al. (2002). In Section 3.3, we allow i and D to vary and consider six disparate dynamical models.

For H1743 and J1550, we only select data over an order of magnitude in luminosity, between $0.05 < L_D/L_{\rm Edd} < 0.5$ for the values of M, i, and D given above. This intermediate range in luminosity is chosen in order to eliminate both hard-state spectra that have little or no detectable thermal component and high-luminosity data for which the thin-disk approximation likely no longer applies. Further requiring goodness of fit (χ^2/ν) < 2 and that the inner radius is well determined ($R_{\rm in}/\Delta R_{\rm in} > 5$, where $\Delta R_{\rm in}$ is the 1σ statistical uncertainty on $R_{\rm in}$) leaves us with a total of 117 spectra for H1743 and 151 spectra for J1550.

We include for KERRBB2 the effects of limb darkening and returning radiation and set the torque at $R_{\rm in}$ to zero (e.g., McClintock et al. 2006), and for the dimensionless viscosity parameter we adopt $\alpha = 0.01$. (Our results in the following section are modestly affected if one instead uses $\alpha = 0.1$: $R_{\rm in}$ is increased by ≈5% and becomes weakly dependent on luminosity, increasing by $\lesssim$10% for an order of magnitude increase in L_D.) A color correction resulting from spectral hardening in the disk atmosphere is internally calculated for KERRBB2 using models KERRBB and BHSPEC (Davis & Hubeny 2006) as described in McClintock et al. (2006). The upscattering-only implementation of SIMPL, known as SIMPL-1, was used exclusively throughout unless otherwise noted. Larger values of $f_{\rm SC}$ are obtained using the double-sided scattering kernel SIMPL-2 (see Table 1), but $R_{\rm in}$ and the other fit parameters are completely unaffected by the choice of kernel.

3. RESULTS

3.1. Final Selection of the Data Via the Scattered Fraction

The scattered fraction $f_{\rm SC}$ sets the strength of the Compton power-law component relative to the disk. Figure 1 shows for H1743 the inner disk radius $R_{\rm in}$ versus $f_{\rm SC}$. For $f_{\rm SC} < 0.25$, the radius is quite stable and its value for the SPL data is very nearly the same as for the TD data. However, at large values of $f_{\rm SC}$ the inner disk radius $R_{\rm in}$ apparently recedes, indicating that either the model breaks down or a real change takes place in the disk. One possible physical explanation was proposed by Done & Kubota (2006), who argue that in regimes of extremely high Comptonization an inner disk corona can truncate the disk and increase $R_{\rm in}$ by tens of percent, consistent with the high values shown in Figure 1.

We have computed and compared plots of $R_{\rm in}$ versus $f_{\rm SC}$ for four BH binaries (H1743, J1550, XTE J1655−40, and LMC X-3) and find that divergent behavior in their values of $R_{\rm in}$ sets in for $f_{\rm SC} \gtrsim 0.2$–0.3 (or $f_{\rm SC} \gtrsim 0.25$–0.4 for SIMPL-2). Based on a consideration of these results, we adopt $f_{\rm SC} < 0.25$ as a data-selection criterion in this work. The application of this criterion leaves a final data sample of 100 spectra for H1743 and 136 for J1550.

3.2. Comparison with Other Comptonization Models

Having applied our Comptonized accretion disk model PHABS (SIMPL ⊗ KERRBB2) and obtained final data samples for H1743 and J1550 (Section 3.1), we now analyze these selected data using alternative models for the Compton com-

Table 1
Comparison of R_{in} Across Spectral States

BH	State	N	$\overline{f_{SC}}$[a]	R_{in} (in $\frac{GM}{c^2}$): KERRBB2 used with		
				SIMPLE-1	POWERLAW	COMPTT[b]
H1743	TD	65	0.012	4.13 ± 0.05	4.10 ± 0.06	4.10 ± 0.07
	INT	2	0.062	$3.79 - 4.10$	$3.48 - 4.02$	$3.73 - 4.08$
	SPL	33	0.135	4.01 ± 0.06	3.10 ± 0.24	3.46 ± 0.27
J1550	TD	100	0.016	5.20 ± 0.06	5.05 ± 0.09	5.14 ± 0.10
	INT	18	0.183	5.16 ± 0.19	4.37 ± 0.57	4.93 ± 0.20
	SPL	18	0.123	5.00 ± 0.15	4.36 ± 0.21	4.91 ± 0.26

Notes. The values and errors quoted for R_{in} are medians and median absolute deviations (MADs); we have chosen these quantities for their robustness. For Gaussian-distributed data, $1\sigma \approx 1.5$ MAD. R_{in} is calculated using the fiducial M, i, and D specified in Section 2.
[a] Calculated for SIMPLE-1. For fits using SIMPL-2, $\overline{f_{SC}}$ is ≈30% larger.
[b] Geometry switch set to 1 (slab geometry) and redshift to 0. All other parameters are left free.

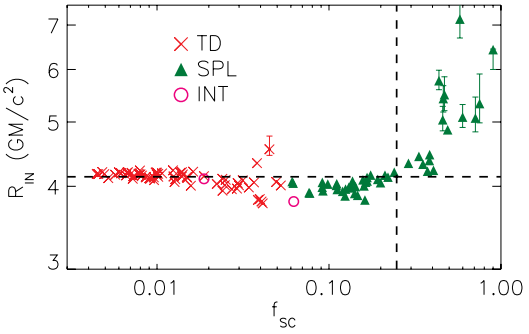

Figure 1. Inner disk radius R_{in} vs. the scattered fraction f_{SC} for H1743. As indicated in the legend, the symbol types denote X-ray state (see Remillard & McClintock 2006). For $f_{SC} < 0.25$, which is our adopted selection criterion, R_{in} is generally constant; the median value for the TD-state data alone is indicated by the dashed line. However, for larger values of f_{SC}, to the right of the vertical dashed line, the values of R_{in} diverge. Results are shown for all 117 spectra with $\chi^2/\nu < 2$ and $R_{in}/\Delta R_{in} > 5$ over the range $L_D = 5\%$–50% L_{Edd} (see Section 2). Error bars (1σ) on R_{in} that are smaller than the plotting symbols have been omitted for clarity. Error bars on f_{SC} are not shown; they are smaller than the plotting symbols except for extreme values of f_{SC} (<0.02 and >0.6).

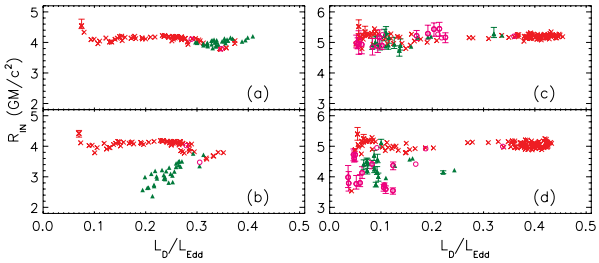

Figure 2. Inner disk radius R_{in} vs. the Eddington-scaled disk luminosity L_D/L_{Edd} for H1743 (left) and J1550 (right). Symbol types are defined in Figure 1. For the upper pair of panels the Comptonization model employed is SIMPL, and for the lower panels it is POWERLAW. The data sample considered here is that described in Section 3.1. For J1550, note in panel (c) the many INT-state data that are brought into agreement with the SPL- and TD-state data when applying SIMPL. Error bars are omitted when smaller than the symbols.

ponent. We employ (1) COMPTT, a widely used model of Comptonization that describes the upscattering of blackbody-like radiation by coronal electrons (Titarchuk 1994), and (2) the empirical model POWERLAW. The full model formulations are respectively PHABS(KERRBB2 + COMPTT) and PHABS (KERRBB2 + POWERLAW). We now use these models to derive values of R_{in} for both sources and compare these results to those obtained using our model.

Figure 2 shows a side-by-side comparison of H1743 (left panels) and J1550 (right panels), where R_{in} is now plotted versus L_D/L_{Edd} (Section 2). The results in the upper pair of panels were obtained using our self-consistent Comptonization model SIMPL, while those in the lower panels were obtained using POWERLAW. Plainly, for both sources SIMPL harmonizes the extreme discord between the SPL/intermediate (INT) data and the TD data that results from analyzing these data using POWERLAW (Figures 2(b) and (d)). The reconciliation achieved using SIMPL (Figures 2(a) and (c)) indicates that the inner disk radii determined in the weakly Comptonized TD state are very nearly the same as in the moderately Comptonized INT and SPL states. Only data matching the selection criteria in Sections 2 and 3.1 are considered.

Table 1 provides a summary of the results shown in Figure 2 and extends the comparison by including results for COMPTT. Qualitatively, the results for both sources are very similar; here we comment only on the results for H1743. Comparing SIMPL with POWERLAW, we see that for the former model R_{in} is consistent between the TD and SPL states, 4.13 ± 0.05 and 4.01 ± 0.06, respectively (values and errors here are the median and median absolute deviation). On the other hand, POWERLAW delivers a radius for the SPL state that is ≈24% smaller than for the TD state: 3.10 ± 0.24 versus 4.10 ± 0.06. While POWERLAW fails dramatically to reconcile the TD- and SPL-state data, COMPTT provides only a modest improvement, giving an ≈16% smaller value of R_{in} for the SPL state: 3.46 ± 0.27 versus 4.10 ± 0.07. The failure of COMPTT and POWERLAW to deliver a constant radius occurs because these additive models compete with the disk component for thermal flux and because they make no allowance for the flux which the disk contributes to the power law.

3.3. Dependence on the Dynamical Model

So far, our results are based on the specific and rather arbitrary dynamical model defined for each source in Section 2. We now demonstrate that the quality of our results does not depend on the choice of a particular triplet of M, i, and D. For H1743, we analyze the data for six disparate dynamical models chosen as follows: we fix the mass at $M = 10\ M_\odot$ and vary the inclination from $i = 30°$ to $i = 80°$ in $10°$ increments, adjusting the distance in order to maintain the peak disk luminosity at $L_D/L_{Edd} \approx 0.7$; this prescription leaves our selection criteria (Sections 2 and 3.1) largely unaffected. For this demonstration, we restrict ourselves to a contiguous set of pristine data that are free of both edge and line features (see McClintock et al. 2009).

Figure 3(a) shows a portion of the 2003 outburst light curve of H1743. Figure 3(b) shows corresponding values of R_{in} versus time for the six models described above. We draw the following key conclusions from Figure 3: (1) R_{in} is constant for each model to within ≈2% as the source passes from the SPL state to the

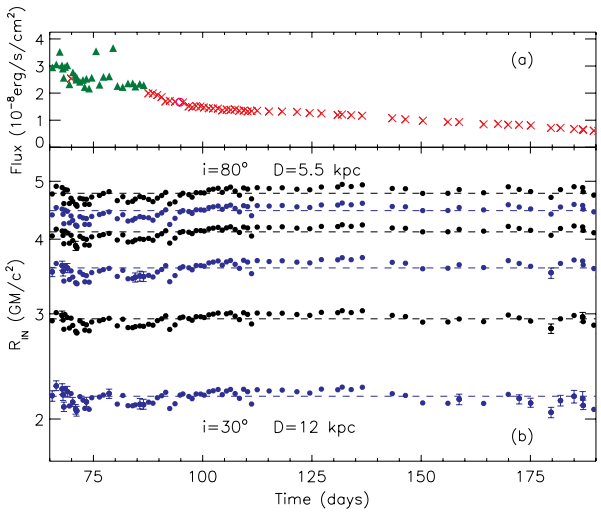

Figure 3. (a) Contiguous 126 day portion of the 225 day *RXTE* PCA light curve of H1743, which is shown in full in Figure 3(a) of McClintock et al. (2009). The 2–20 keV unabsorbed fluxes were obtained by modeling the PCA spectral data. Time zero is the date of discovery of H1743 during its 2003 outburst, which occurred on 2003 March 21 (MJD 52719). (b) $R_{\rm in}$ vs. time for the six models described in the text, shown as alternating black/blue tracks for clarity. The median absolute deviations for the extreme models with $i = 30°$ and $i = 80°$ are 2.2% and 1.8%, respectively. Fluxes for 83 spectra are plotted in panel (a) and 79 values of $R_{\rm in}$ are plotted in panel (b) (except for $i = 40°$ with 78); i.e., four (five for $i = 40°$) spectra failed to meet our selection criteria. Error bars are omitted where they are smaller than the symbols.

TD state, and as the source flux decays by a factor of ≈6. We furthermore note that $R_{\rm in}$ is stable during the two strong SPL-state flares that occur on days 75.6 and 79.5. (2) The character of the small systematic variations that occur in $R_{\rm in}$ during this entire 4-month period are essentially the same for all six models. For completeness, we recomputed all the results shown in Figure 3(b) using first $M = 5\ M_\odot$ and then $M = 15\ M_\odot$. Apart from offsetting the value of $R_{\rm in}$, the character of these results is the same, including the level of scatter, as for the case of $M = 10\ M_\odot$. We conclude that, apart from setting the median value of $R_{\rm in}$, the choice of model has no significant effect on the results presented in Figure 3.

Likewise, for J1550 we analyzed a ∼130 day stretch of data obtained during the 1998 outburst cycle (MJD 51110−51242; Sobczak et al. 2000). We assumed fiducial values of M and i and explored a wide range of distances from $D = 3$–8 kpc. We obtained results very similar to those presented for H1743 (Figure 3(b)), consistent with an internal scatter of ≈2%.

4. DISCUSSION

Kubota et al. (2001) and Kubota & Makishima (2004) present the first self-consistent treatment of disk-dominated accretion at high luminosity in BH binaries. They showed for GRO J1655−40 and J1550 that what previously had appeared to be anomalous behavior was a natural result of strong inverse-Compton scattering. In particular, they demonstrated that the inner disk radius was stable when the flux attributed to the power law was properly associated with the disk. Their results have been confirmed recently by Steiner et al. (2009) using SIMPL (Sections 1 and 2). In this Letter, we provide additional support for the work of Kubota et al., while supplying in this context the first relativistic analysis of the accretion disk component. Both the earlier work by Kubota et al. and this Letter demonstrate that, when modeling Comptonization, a self-consistent treatment is necessary in order to explain BH behavior across spectral states.

In all of our earlier work measuring the spins of BHs using KERRBB2, we have selected data with $L_D/L_{\rm Edd} < 0.3$, which corresponds to the thin-disk limit ($H/R \lesssim 0.1$; McClintock et al. 2006). In the present work, the luminosity of J1550 is very uncertain and that of H1743 is unconstrained. For this reason, we present a broad range of luminosities, which likely exceeds the thin-disk limit. In work aimed at determining BH spin, when reliable distance estimates and dynamical data are available, one should apply the aforementioned luminosity restriction.

In conclusion, we have analyzed a selected sample of ∼100 spectra for each of two bright transient sources using the self-consistent Comptonization model SIMPL convolved with a relativistic accretion disk model. We have thereby shown that the derived inner disk radii—or, equivalently, the derived spins of these BHs—remain stable to a few percent whether the source is in the TD state or the more strongly Comptonized SPL state. We have further shown that this stability holds for $f_{\rm SC} \lesssim 0.25$ and for a wide range of input model parameters. We conclude that the CF method of estimating BH spin can be applied to far more X-ray spectral data and more sources than previously thought possible.

The authors thank Jifeng Liu for valuable discussions. J.F.S. was supported by the Smithsonian Institution Endowment Funds and J.E.M. acknowledges support from NASA grant NNX08AJ55G. R.N. acknowledges support from NASA grant NNX08AH32G and NSF grant AST-0805832. R.A.R. acknowledges partial support from the NASA contract to MIT for support of *RXTE* instruments.

REFERENCES

Arnaud, K. A. 1996, in ASP Conf. Ser. 101, Astronomical Data Analysis Software and Systems V, ed. G. H. Jacoby & J. Barnes (San Francisco, CA: ASP), 17
Brenneman, L. W., & Reynolds, C. S. 2006, ApJ, 652, 1028
Davis, S. W., & Hubeny, I. 2006, ApJS, 164, 530
Done, C., & Kubota, A. 2006, MNRAS, 371, 1216
Gou, L., McClintock, J. E., Liu, J., Narayan, R., Steiner, J. F., Remillard, R. A., Orosz, J. A., & Davis, S. W. 2009, ApJ, 701, 1076
Jahoda, K., Markwardt, C. B., Radeva, Y., Rots, A. H., Stark, M. J., Swank, J. H., Strohmayer, T. E., & Zhang, W. 2006, ApJS, 163, 401
Kubota, A., & Makishima, K. 2004, ApJ, 601, 428
Kubota, A., Makishima, K., & Ebisawa, K. 2001, ApJ, 560, L147
Li, L.-X., Zimmerman, E. R., Narayan, R., & McClintock, J. E. 2005, ApJS, 157, 335
Liu, J., McClintock, J. E., Narayan, R., Davis, S. W., & Orosz, J. A. 2008, ApJ, 679, L37
McClintock, J. E., Remillard, R. A., Rupen, M. P., Torres, M. A. P., Steeghs, D., Levine, A. M., & Orosz, J. A. 2009, ApJ, 698, 1398
McClintock, J. E., Shafee, R., Narayan, R., Remillard, R. A., Davis, S. W., & Li, L.-X. 2006, ApJ, 652, 518
Miller, J. M., Reynolds, C. S., Fabian, A. C., Miniutti, G., & Gallo, L. C. 2009, ApJ, 697, 900
Miller, J. M., et al. 2003, MNRAS, 338, 7
Miniutti, G., et al. 2007, PASJ, 59, 315
Orosz, J. A., et al. 2002, ApJ, 568, 845
Remillard, R. A., & McClintock, J. E. 2006, ARA&A, 44, 49
Shafee, R., McClintock, J. E., Narayan, R., Davis, S. W., Li, L.-X., & Remillard, R. A. 2006, ApJ, 636, L113
Shapiro, S. L., & Teukolsky, S. A. 1983, Black Holes, White Dwarfs, and Neutron Stars (New York: Wiley Interscience)
Sobczak, G. J., McClintock, J. E., Remillard, R. A., Cui, W., Levine, A. M., Morgan, E. H., Orosz, J. A., & Bailyn, C. D. 2000, ApJ, 544, 993
Steiner, J. F., Narayan, R., McClintock, J. E., & Ebisawa, K. 2009, PASP, submitted (arXiv:0810.1758v2)
Swank, J. H. 1999, Nucl. Phys. B Proc. Suppl., 69, 12
Tanaka, Y., et al. 1995, Nature, 375, 659
Titarchuk, L. 1994, ApJ, 434, 570
Toor, A., & Seward, F. D. 1974, AJ, 79, 995
Zhang, S. N., Cui, W., & Chen, W. 1997, ApJ, 482, L155